ChemComm

Peptide Pigments Inside Liquid Droplets Through Confined Enzymatic Oxidation

Journal:	*ChemComm*
Manuscript ID	CC-COM-08-2023-004231.R1
Article Type:	Communication

COMMUNICATION

Peptide Pigments Inside Liquid Droplets Through Confined Enzymatic Oxidation

Received 00th January 20xx,
Accepted 00th January 20xx

DOI: 10.1039/x0xx00000x

Kenny Barriales,[a-c] Salma Kassem,[a] Deborah Sementa,[a] Alfredo Vidal Ceballos,[a,c] Tong Wang,[a] Shadman Khandaker,[a] Rinat R. Abzalimov,[a] Ankit Jain,[a,d] Shana Elbaum-Garfinkle[a,c] and Rein V. Ulijn[a-c]

Melanin pigments are found in most life forms, where they are responsible for coloration and ultraviolet (UV) light protection. Natural melanin is a poorly soluble and complex biosynthesis product produced through confined and templated enzymatic oxidation of tyrosine. It has been challenging to create water-soluble synthetic mimics. This study demonstrates the enzymatic synthesis of oxidized phenols confined inside liquid droplets. We use an amphiphilic, bifunctional peptide, $DYFR_9$, that combines a tyrosine tripeptide previously shown to undergo enzymatic oxidation to form peptide pigments with broad absorbance, and polyarginine to facilitate complex coacervation in presence of ATP. When ATP, $DYFR_9$ are mixed and exposed to tyrosinase, pigmented liquid droplets result, while no appreciable oxidation is observed in the bulk.

Melanin is a natural biopolymer with remarkable properties including UV-protection, coloration, and antioxidant activity.[1] Natural melanin synthesis is a complex multi-step process involving catalyic oxidation, templating, and oxidation under confinement.[2–4] While they are promising for technical applications, the usefulness of this class of materials is constrained by their makeup of heterogeneous products, which are typically insoluble polymers with ill-defined chemical and structural compositions.[5] These obstacles have motivated efforts to create synthetic materials that mimic and resemble the UV-aborptive properties of melanin.[2,6,7] The majority of these mimetic compounds are based on polydopamine derivatives that are produced *via* oxidative polymerization of phenols, such as dopamine or tyrosine.[8–11] The resulting brown-bleck materials display are chemically heterogenous and remain poorly soluble. The use of tyrosine-containing short peptides as precursor templates for enzymatic oxidation, and formation of polymeric pigments has been explored and begins with the enzymatic oxidation of L-tyrosine to 3,4-dihydroxyphenylalanine (L-DOPA).[6,7,12,13] Self-assembly of short peptides containing one or more aromatic residues (frequently including tyrosine) has been studied extensively.[14] By editing the sequence of self-assembling tyrosine containing tripeptides followed by enzymatic oxidation, unique architectures not known in nature become accessible, such as 2D sheets,[6] and 1D nanofibrous[12] polymeric peptide pigments with remarkable optical[7] and conductive[12] properties. These studies demonstrate the potential of peptide self-assembly and enzymatic oxidation to direct formation of laboratory-based synthetic melanin analogs.[15]

Biomolecular condensates formed through liquid-liquid phase separation (LLPS) have emerged as a thriving area of research due to their recognized importance in life sciences,[16] including marine biology,[17] and cellular biochemistry.[18] Relevant to the current study, liquid condensates have been implicated in formation of adhesives and DOPA materials from mussel foot proteins.[19] Furthermore, condensates have shown to play a crucial role in regulating cellular processes and signaling pathways, including through serving as biomolecular scaffolds for enzymatic reactions.[20]

Following this surge of interest in fundamental understanding and materials applications of biological LLPS as a space/time regulatory mechanism in biological systems, the use of LLPS has been used to spatiallly control enzymatic oxidation reactions. Lampel's group demonstrated the use of polyethylene glycol/dextran aqueous two-phase system with a photocleavable protected tyrosine, which gave rise to oxidized tyrosine induced in a LLPS system.[21] In this system, the condensates served as a reaction vessel in which tyrosine can be oxidized.[21] Using short peptiddes have also been recognized to forrm short peptides.[22]

[a] *Advanced Science Research Center (ASRC) at the Graduate Center, City University of New York (CUNY), 85 St Nicholas Terrace, New York, New York 10031, United States.*
[b] *Department of Chemistry, Hunter College, City University of New York, 695 Park Avenue, New York, New York 10065, United States.*
[c] *Ph.D. Program in Chemistry, The Graduate Center of the City University of New York, New York, New York 10016, United States.*
[d] *Department of Chemistry and biochemistry, Brooklyn College, City University of New York, 2900 Bedford Avenue, Brooklyn, NY 11210, United States.*
Electronic Supplementary Information (ESI) available: [details of any supplementary information available should be included here]. See DOI: 10.1039/x0xx00000x

Here, it was our objective to control the generation of melanin mimics in a LLPS system where the tyrosine residues are themselves a structural part of the condensates. The foundation of our design is an amphiphilic peptide, Ac-DYFR$_9$, that is composed of a tripeptide known to form polymeric pigments with broad UV absorbance upon enzymatic oxidation, DYF,[6] and a polyarginine component that was designed to facilitate complex coacervation with ATP (Figure 1A).[23] The design builds on recently demonstrated amphiphilic peptides that combine the features of fibrous self-assembly and complex coacervation by creating fused peptides that combine a beta-sheet forming domain (LVFFA) with a coacervation motif (oligoarginine and ATP) have been explored to create supramolecular fibers exclusively inside defined compartments (LVFFAR$_9$/ATP).[24] Our intention was to exploit the assembly of DYF, and complex coacervation of R$_9$/ATP, in order to obtain templated self-assembly inside condensates, and furthermore to form particles or droplets that remain dispersed upon enzymatic oxidation in aqueous buffer.[6]

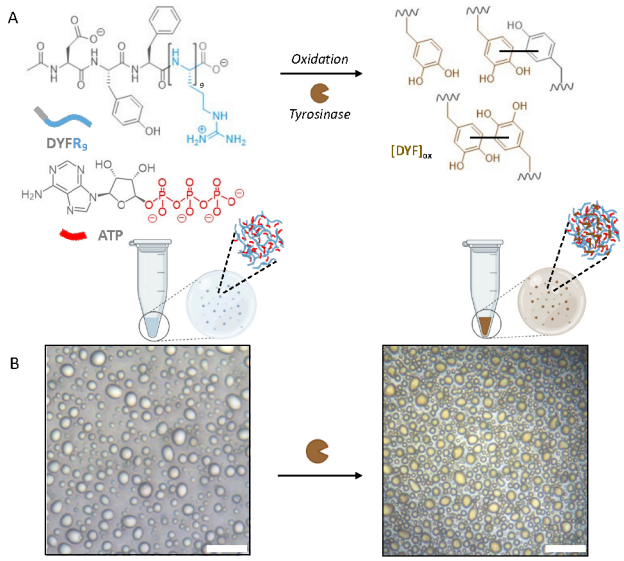

Figure 1 - Design of peptide pigment synthesis in liquid droplets. (A) Molecular structures of the polymeric peptide sequence that is used for the formation of coacervates with ATP. (B) Optical microscope images of the oxidative polymerization-induced pigment synthesis in liquid droplets after the conjugation of the tyrosine containing peptide DYFR$_9$ with ATP. Scale bar = 20 μm.

Upon mixing 1mM Ac-DYFR$_9$ and 25 mM ATP solutions, liquid-liquid phase seperation occurred and colorless coacervates were observed under optical microscopy (Figure 1A). The pH of the mixtures was maintained at 7.0 buffered by 10 mM Tris HCl containing 15 mM KCl, 0.5 mM $MgCl_2$, and 0.2% (w/v) NaN_3. The samples were imaged through sandwiched 1 mm spaced, surface-functionalized (with *N*-(triethoxysilylpropyl)-*O*-poly(ethylene oxide)) glass slides to reduce coalescence of droplets on glass surface.[25,26] Following this coacervation, we then added 5 mg/mL mushroom tyrosinase to the coacervate mixture to induce a tyrosine oxidation. After one hour at 20°$\boldsymbol{C}$ – 30°$\boldsymbol{C}$, this gave rise to brown colored coacervates indicative of compartmentalization of melanin formation in the droplets (Figure 1B).

In order to confirm the liquid-like properties of these structures, we further characterized droplets with flourescence recovery after photobleaching (FRAP) (Dye: 0.5% *f*-ATP, Figure 2C). There was no difference in flourescent recovery after one hour of incubation (Figure 2C). This behavior is consistent with the liquid-like dynamics inside the droplets even after one hour of oxidation. In addition, we captured snapshots and videos of the FRAP process on coacervates to illustrate the fluorescent recovery at the t = 1h time point (Figure 2A, Movie S1). Furthermore, our investigations reveal that these tyrosine-induced droplets have the tendency to coalesce, resulting in the formation of larger droplets over time (Figure 2B). This observation further supports the liquid-like nature of these coacervates post oxidation. Beyond t = 1h the droplets then begin to settle. The use of cryo-transmission electron microscopy (Cryo-TEM) has allowed us to confirm minimal morphological changes of the coacervates containing oxidized peptide. We note that there was no evidence of fibrous peptide self-assembly as previously observed for the LVFFA system,[24] presumably due to the reduced 1D self-assembly propensity of the DYF peptide, and the disrupting nature of the R$_9$ appendages. Additional images were provided (Figure 2D, Figure S1).

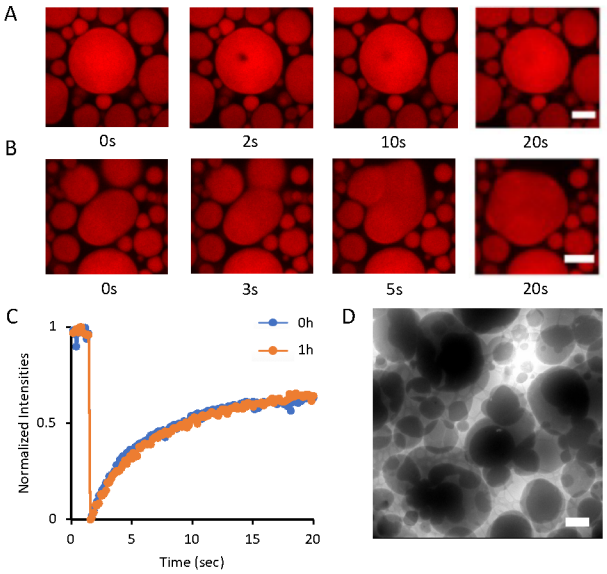

Figure 2 - Fluorescence recovery after photobleaching of oxidized droplets. A) Confocal images corresponding to FRAP in coacervates at t = 1h after oxidation. Scale bar = 5 μm. (B) Confocal images showing droplet merge over the course of 20s. Scale bar = 5 μm. (C) FRAP traces of oxidized DYFR$_9$ droplets using 0.5% *f*-ATP dye. (D) Cryo-TEM image of DYFR$_{9\,ox}$ coacervates. Scale bar = 2 μm

To monitor chemical oxidation inside coacervates using UV/Visible and mass spectroscopy, we centrifuged the coacervates mixture to separate the condensate phase from the buffer solution. Separating the two phases post-oxidation gave rise to poorly reproducible results because the centrifugation process itself gave rise to crossover of the enzymes between the two phases, resulting in additional oxidation. So instead, we separated the mixtures prior to oxidation using centrifugation, and the enzyme was then added to both phases at the identical final concentration (Figure 3A) and the oxidation was followed by UV-vis spectroscopy. We observed increases in broad absorbance as evidence of oxidation predominantly inside the DYFR$_9$ droplets. A separate (disconnected) DYF-NH$_2$ (1 mM) and R$_9$ (1 mM) mixture was used as a control

experiment. In this case, we see low levels of oxidation of DYF + R_9 in droplets (Figure 3B, ii2). At 3 hours, the intensity difference has increased by more than 3.5 times in the supernatant (Figure 3B, ii1) demonstrating that the tripeptide was most abundant outside of the condensate phase. After 3 hours of oxidation, images of the reaction tubes were taken to illustrate the development of brown color in the supernatant, and no coloration was observed visually in the condensate phase. In contrast, higher absorbance intensity was observed for tyrosine oxidation in the $DYFR_9$ droplets. In this case, oxidation of $DYFR_9$ in the condensate phase showed an absorbance intensity increase that was 5 times enhanced (Figure 3B, i2) compared to the supernatant (Figure 3B, i1). Images of the reaction tubes were taken after 3 hours of oxidation to show the development of brown color in the droplet phase, but no brown color was visible in the supernatant phase. In addition, droplets containing oxidized tyrosine showed intrinsic fluorescent emission upon excitation at λ= 405 nm.[21] As expected, fluorescence intensity of oxidized $DYFR_9$ was significantly higher compared to its surroundings (Figure S2). We can conclude that production of oxidized peptide pigments within coacervates is conceivable using an amphiphilic peptide that contains both a tyrosine-containing motif and a complex coacervate system. Our findings align with previously established literature that has measured tyrosine oxidation products using UV-vis,[6,7,27,28] and tyrosine oxidation within coacervates.[21]

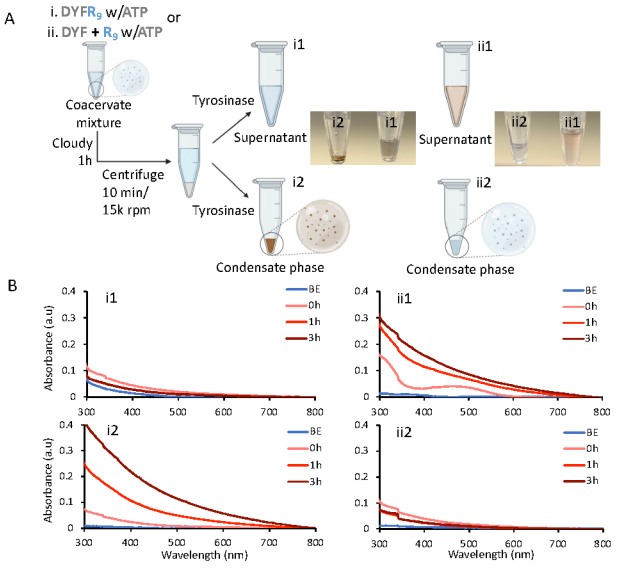

Figure 3 - Tyrosine oxidation within coacervates. (A) Schematic showing the separation process of the biphasic mixture of $DYFR_9$ (i) and DYF + R_9 (ii) to which UV-Vis spectra was collected. Reaction tube images of the corresponding reaction after t = 3h. (B) UV-Vis absorption spectra in the broad absorption range (300-800nm). Oxidation of the experimental, $DYFR_9$ in the supernatant (i1) and in the condensate phase (i2). Oxidation of the control DYF + R_9 in the supernatant (ii1) and in the condensate phase (ii2). BE = Before Enzyme addition, t = 0h (within one minute of adding enzyme), t = 1h, and t = 3h (one and three hours after enzyme was added).

Matrix Assisted Laser Desorption/Ionization (MALDI) was used to analyze and confirm tyrosine oxidation. Tyrosine-containing peptides undergo polymerization in which change in molecular weight is observed after oxidation, which can be visualized through MALDI.[6,29] The most prominant peak observed from MALDI is the DOPA form of the peptide, which is a crucial intermediate in the melanin synthesis pathway resulting from the oxidation of tyrosine (Figure S3). A low degree of cross-linking was observed in the mass spectra of the oxidized peptide by the presence of oxidized dimers (Figure S3), which is likely responsible for the brown color observed. MALDI was also analyzed for the various disconnected DYF+R_9 sequences including their interaction with ATP to assure DOPA and polymer formation from the DYF domain (Figure S4). Liquid Chromotagraphy-Mass Spectrometry (LCMS) was also utilized for further characterization of the oxidized products. We performed a chymotrypsin hydrolysis[30,31] in order to remove R_9 from the Ac-$DYFR_9$ peptide which allowed the retention of the tripeptide and its oxidized products on the column (Figure S5-S8). While we are unable to fully characterize this mixture, the results confirm that the tripeptide DOPA catechol and quinone are formed, and we propose that the repulsion of R_9 tails and the liquid nature of the materials prevents oligomerization that was observed in free peptide systems reported previously.[6]

Our study has demonstrated the feasibility of using a multicomponent peptide sequence that utilizes designed constituents to promote the formation of melanin mimetic compounds within coacervates. One of the main challenges in formation of melanin-mimetics has been to confine the reaction product in the condensed phase, which our design effectively addresses. Furthermore, our findings shed light on potential strategies for controlling the unregulated synthesis of insoluble biopolymers. Mimicking melanin with synthetic materials can benefit individuals with melanin deficiency. The implications of this research extend beyond the laboratory, as it has the potential to lead to sun protection applications relevant to cosmetics.

A.J. and S.K. conceived the idea. K.B., A.J., S.K., and R.V.U. designed the study. K.B. performed the experimental methodology and data analysis. A.V.C. performed the FRAP experiment. D.S. performed fluorescence measurements. T.W. performed the Cryo-TEM experiment. K.B. and R.V.U. wrote the manuscript with input from A.J., S.K., D.S., S.Kh., A.V.C. and S.E.G.

Acknowledgements

R.V.U. acknowledges funding from Office of Naval Research for the Vannevar Bush Faculty Fellowship (Grant No. N00014-21-1-2967). We thank the Air Force Office of Scientific Research for funding of R.V.U. and K.B (Grant No. FA9550-21-1-0091)

Conflicts of interest

There are no conflicts to declare.

Notes and references

(1) Liu, B.-W.; Huang, P.-C.; Li, J.-F.; Wu, F.-Y. Colorimetric Detection of Tyrosinase during the Synthesis of Kojic Acid/Silver Nanoparticles under Illumination. *Sens. Actuators B Chem.* **2017**, *251*, 836–841.

(2) Cao, W.; Zhou, X.; McCallum, N. C.; Hu, Z.; Ni, Q. Z.; Kapoor, U.; Heil, C. M.; Cay, K. S.; Zand, T.; Mantanona, A. J.; Jayaraman, A.; Dhinojwala, A.; Deheyn, D. D.; Shawkey, M. D.; Burkart, M. D.; Rinehart, J. D.; Gianneschi, N. C. Unraveling the Structure and Function of Melanin through Synthesis. *J. Am. Chem. Soc.* **2021**, *143* (7), 2622–2637.

(3) Meredith, P.; Sarna, T. The Physical and Chemical Properties of Eumelanin. *Pigment Cell Res.* **2006**, *19* (6), 572–594.

(4) El-Naggar, N. E.-A.; Saber, W. I. A. Natural Melanin: Current Trends, and Future Approaches, with Especial Reference to Microbial Source. *Polymers* **2022**, *14* (7), 1339.

(5) d'Ischia, M.; Napolitano, A.; Ball, V.; Chen, C.-T.; Buehler, M. J. Polydopamine and Eumelanin: From Structure–Property Relationships to a Unified Tailoring Strategy. *Acc. Chem. Res.* **2014**, *47* (12), 3541–3550.

(6) Lampel, A.; McPhee, S. A.; Park, H.-A.; Scott, G. G.; Humagain, S.; Hekstra, D. R.; Yoo, B.; Frederix, P. W. J. M.; Li, T.-D.; Abzalimov, R. R.; Greenbaum, S. G.; Tuttle, T.; Hu, C.; Bettinger, C. J.; Ulijn, R. V. Polymeric Peptide Pigments with Sequence-Encoded Properties. *Science* **2017**, *356* (6342), 1064–1068.

(7) Lampel, A.; McPhee, S. A.; Kassem, S.; Sementa, D.; Massarano, T.; Aramini, J. M.; He, Y.; Ulijn, R. V. Melanin-Inspired Chromophoric Microparticles Composed of Polymeric Peptide Pigments. *Angew. Chem. Int. Ed.* **2021**, *60* (14), 7564–7569.

(8) Cavallini, C.; Vitiello, G.; Adinolfi, B.; Silvestri, B.; Armanetti, P.; Manini, P.; Pezzella, A.; d'Ischia, M.; Luciani, G.; Menichetti, L. Melanin and Melanin-Like Hybrid Materials in Regenerative Medicine. *Nanomaterials* **2020**, *10* (8), 1518.

(9) Battistella, C.; McCallum, N. C.; Gnanasekaran, K.; Zhou, X.; Caponetti, V.; Montalti, M.; Gianneschi, N. C. Mimicking Natural Human Hair Pigmentation with Synthetic Melanin. *ACS Cent. Sci.* **2020**, *6* (7), 1179–1188.

(10) Lee, H.; Dellatore, S. M.; Miller, W. M.; Messersmith, P. B. Mussel-Inspired Surface Chemistry for Multifunctional Coatings. *Science* **2007**, *318* (5849), 426–430.

(11) Tian, Z.; Wu, G.; Libby, M.; Wu, K.; Jeong, K. J.; Kim, Y. J. Synthesis of Biologically Derived Poly(Pyrogallol) Nanofibers for Antibacterial Applications. *J. Mater. Chem. B* **2023**, *11* (15), 3356–3363.

(12) Reddy, S. M. M.; Raßlenberg, E.; Sloan-Dennison, S.; Hesketh, T.; Silberbush, O.; Tuttle, T.; Smith, E.; Graham, D.; Faulds, K.; Ulijn, R. V.; Ashkenasy, N.; Lampel, A. Proton-Conductive Melanin-Like Fibers through Enzymatic Oxidation of a Self-Assembling Peptide. *Adv. Mater.* **2020**, *32* (46), 2003511.

(13) Wang, Z.; Tschirhart, T.; Schultzhaus, Z.; Kelly, E. E.; Chen, A.; Oh, E.; Nag, O.; Glaser, E. R.; Kim, E.; Lloyd, P. F.; Charles, P. T.; Li, W.; Leary, D.; Compton, J.; Phillips, D. A.; Dhinojwala, A.; Payne, G. F.; Vora, G. J. Melanin Produced by the Fast-Growing Marine Bacterium Vibrio Natriegens through Heterologous Biosynthesis: Characterization and Application. *Appl. Environ. Microbiol.* **2020**, *86* (5), e02749-19.

(14) Frederix, P. W. J. M.; Scott, G. G.; Abul-Haija, Y. M.; Kalafatovic, D.; Pappas, C. G.; Javid, N.; Hunt, N. T.; Ulijn, R. V.; Tuttle, T. Exploring the Sequence Space for (Tri-)Peptide Self-Assembly to Design and Discover New Hydrogels. *Nat. Chem.* **2015**, *7* (1), 30–37.

(15) Riley, P. A. Melanin. *Int. J. Biochem. Cell Biol.* **1997**, *29* (11), 1235–1239.

(16) Yewdall, N. A.; André, A. A. M.; Lu, T.; Spruijt, E. Coacervates as Models of Membraneless Organelles. *Curr. Opin. Colloid Interface Sci.* **2021**, *52*, 101416.

(17) Astoricchio, E.; Alfano, C.; Rajendran, L.; Temussi, P. A.; Pastore, A. The Wide World of Coacervates: From the Sea to Neurodegeneration. *Trends Biochem. Sci.* **2020**, *45* (8), 706–717.

(18) Banani, S. F.; Lee, H. O.; Hyman, A. A.; Rosen, M. K. Biomolecular Condensates: Organizers of Cellular Biochemistry. *Nat. Rev. Mol. Cell Biol.* **2017**, *18* (5), 285–298.

(19) Kaminker, I.; Wei, W.; Schrader, A. M.; Talmon, Y.; Valentine, M. T.; Israelachvili, J. N.; Waite, J. H.; Han, S. Simple Peptide Coacervates Adapted for Rapid Pressure-Sensitive Wet Adhesion. *Soft Matter* **2017**, *13* (48), 9122–9131.

(20) Zhang, Y.; Narlikar, G. J.; Kutateladze, T. G. Enzymatic Reactions inside Biological Condensates. *J. Mol. Biol.* **2021**, *433* (12), 166624.

(21) Massarano, T.; Baruch Leshem, A.; Weitman, M.; Lampel, A. Spatiotemporal Control of Melanin Synthesis in Liquid Droplets. *ACS Appl. Mater. Interfaces* **2022**, *14* (18), 20520–20527.

(22) Donau, C.; Späth, F.; Stasi, M.; Bergmann, A. M.; Boekhoven, J. Phase Transitions in Chemically Fueled, Multiphase Complex Coacervate Droplets. *Angew. Chem. Int. Ed.* **2022**, *61* (46), e202211905.

(23) Fisher, R. S.; Elbaum-Garfinkle, S. Tunable Multiphase Dynamics of Arginine and Lysine Liquid Condensates. *Nat. Commun.* **2020**, *11* (1), 4628.

(24) Jain, A.; Kassem, S.; Fisher, R. S.; Wang, B.; Li, T.-D.; Wang, T.; He, Y.; Elbaum-Garfinkle, S.; Ulijn, R. V. Connected Peptide Modules Enable Controlled Co-Existence of Self-Assembled Fibers Inside Liquid Condensates. *J. Am. Chem. Soc.* **2022**, *144* (33), 15002–15007.

(25) Mountain, G. A.; Keating, C. D. Formation of Multiphase Complex Coacervates and Partitioning of Biomolecules within Them. *Biomacromolecules* **2020**, *21* (2), 630–640.

(26) Kaur, T.; Raju, M.; Alshareedah, I.; Davis, R. B.; Potoyan, D. A.; Banerjee, P. R. Sequence-Encoded and Composition-Dependent Protein-RNA Interactions Control Multiphasic Condensate Morphologies. *Nat. Commun.* **2021**, *12* (1), 872.

(27) Ha, D.; Kang, K. Nucleophilic Regulation of the Formation of Melanin-like Species by Amyloid Fibers. *ACS Omega* **2022**, *7* (1), 773–779.

(28) Shin, J. H.; Le, N. T. K.; Jang, H.; Lee, T.; Kang, K. Supramolecular Regulation of Polydopamine Formation by Amyloid Fibers. *Chem. – Eur. J.* **2020**, *26* (24), 5500–5507.

(29) Brennan, M. J.; Kilbride, B. F.; Wilker, J. J.; Liu, J. C. A Bioinspired Elastin-Based Protein for a Cytocompatible Underwater Adhesive. *Biomaterials* **2017**, *124*, 116–125.

(30) Kumar, M.; Sementa, D.; Narang, V.; Riedo, E.; Ulijn, R. V. Self-Assembly Propensity Dictates Lifetimes in Transient Naphthalimide–Dipeptide Nanofibers. *Chem. – Eur. J.* **2020**, *26* (38), 8372–8376.

(31) Duan, Y. J.; Laursen, R. A. Protease Substrate Specificity Mapping Using Membrane-Bound Peptides. *Anal. Biochem.* **1994**, *216* (2), 431–438.